정보저장시스템학회논문집, 제 1 권 제 2 호, pp.137~142

A New Approach to Servo System Design in Hard Disk Drive Systems

Nam-Guk Kim†, Soo-Young Choi*, Sang-Hoon Chu*, Kang-Seok Lee*, and Ho-Seong Lee*

Abstract

In this paper, we propose a new servo system design strategy to reduce the position error signal(PES) and track mis-registration(TMR) in magnetic disk drive systems. The proposed method provides a systematic design procedure based on the plant model and an optimal solution via an optimization with a "Robust Random Neighborhood Search (RRNS)" algorithm. In addition, it guarantees the minimum PES level as well as stability to parametric uncertainties. Furthermore, the proposed method can be used to estimate the performance at the design stage and thus can reduce the cost and time for the design of the next generation product. The reduction of PES as well as robust stability is demonstrated by simulation and experiments.

Key Words : HDD, Servo, PES, TMR, Stability, Robust Optimization, RRNS.

1. Introduction

Because of the dramatically increasing track density and decreasing form factor in the hard disk drive systems, disk drive manufacturers have to work harder to achieve a higher areal/track density. The rapid increase of the track density has imposed a significant burden on a hard disk drive servo and mechanical system [3][4]. It seems that the achievement of an appropriate TMR level with a reasonable stability margin becomes more and more difficult as the track per inch(TPI) increases. On the other hand, the prediction of the performance of next generation product at the design stage is also strongly desired to reduce the cost and time[4].

In order to reduce the TMR of hard disk drives, increasing the bandwidth of a hard disk drive servo system is the simplest way. Unfortunately however, increasing the bandwidth is also difficult because of the instability due to the mechanical resonances of a head disk assembly (HDA).

Up to now, for the servo loop design, we have relied on a simple double integrator model for the VCM. In some papers, a double integrator with some resonance models is considered but it is also far from the real system[1][3]. On the other hand, we have used a trial and error method to minimize the PES and checked the conventional gain margin and phase margin to guarantee the stability of the overall system[1-4]. However, the lack of information for the precise plant model yields a conservative design and therefore has limited the performance of the whole system.

In order to solve all the above problems, we propose a new systematic controller design procedure and servo parameter optimization method, which guarantee the minimum PES with an adequate stability margin. The proposed method is a frequency domain design procedure which is based on reconstructed disturbance data and the fitted model of each sub-system such as HDA, power amplifier, and so on. Note that we used a number of drives to obtain the mathematical model as well as the disturbance data to guarantee the robustness and the minimum level PES in an average sense. Also note that the disturbance data and mathematical model can be obtained from different sources such as direct model measurement of a disc vibration or a new design by CAD tool, which means that the proposed method can be used for the estimation of the PES level for the next generation product at the design stage[4].

This paper is organized as follows. In chapter 2, a mathematical model of HDD servo systems is derived and the external disturbance is identified. In chapter 3, we formulate our optimization problem and propose a

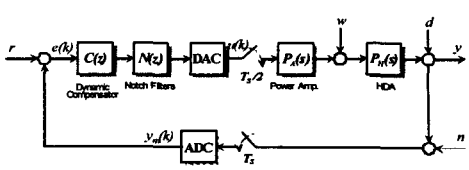

Fig. 1 Block diagram of a HDD servo system

† Storage System Division/Samsung Electronics Co., Ltd.
E-mail : namguk.kim@samsung.com
* Storage System Division/Samsung Electronics Co., Ltd.
논문접수일 (2005 년 4 월 2 일)

RRNS optimization algorithm.In chapter 4, minimization of PES as well as robust stability by the optimized controller is confirmed by both simulation and experiments. Conclusion is given in chapter 5.

2. Preliminary Result

2.1 HDD Servo System

Fig.1 shows a block diagram of hard disk drive servo systems. As is shown in the figure, the HDD servo system consists of HDA($P_H(s)$), power amplifier($P_A(s)$), digital controller(C(z)), notch filter(N(z)), ADC, DAC, and four exogenous inputs(w, d, n, r) and one output(y).

The output y is called PES and r is the reference input which is set to zero during the track following mode. On the other hand, w, d, and n represent the force disturbance, position disturbance, and electrical noise, respectively. The position $y_m(k)$ is measured using ADC at every servo sector and the current command output $u(k)$ by DAC is sent out twice per every servo sector while the controller $C(z)$ is updated once at every servo sector.

2.2 Derivation of a Mathematical Model

In order to optimize the overall performance of the HDD servo systems, we have to know the exact model of the plant. Below, we derive a mathematical model of the HDD servo system shown in Fig.1.

First, we measure the frequency response of HDA and the power amplifier using the laser Doppler vibrometer (LDV) and a dynamic signal analyzer(DSA). Then, we fit the measured data using high order linear system models with a curve fitting tool. In Fig.2, the *Bode* plots of the double integrator model, the plant model with a measurement data, and fitted mathematical model are shown. As is shown in the figure, the fitted model matches the measurement data quite closely while there is a big discrepancy between the double integrator model and the measured data. For the fitted model, 60th order system and 8th order system for the HDA and the power amplifier are used, respectively. Note that Fig.2 shows the frequency response of the system excluding the notch filters, the digital controller, and the sampling effect.

Second, we derive a discretized plant model, which includes digital notch filters, using the fitted models. Multi-rate notch filters $N_m(z)$ as well as conventional single rate notch filters $N_S(z)$ are generally used in HDD servo systems to attenuate the high frequency resonance modes. By applying the single/multi-rate notch filters to

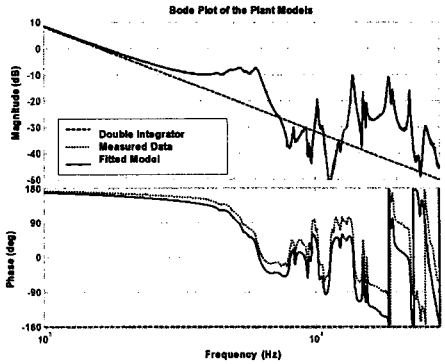

Fig. 2 Bode plot of the plant models

the plant model considering the time delay(T_d), the effect of the zero order hold(ZOH), the decimation effect due to a multi-rate DAC, and a single rate ADC, we can obtain the discretized plant model $G_P(z)$ as followings[2],[5].

$$G_p(z) = \Psi_D\left\{(1-z_2^{-1})\cdot Z\left\{\frac{G_p(s)}{s}e^{-T_d s}\right\}\cdot N_m(z_2),2\right\}\cdot N_s(z) \quad (1)$$

Here,

$$G_p(s)=tpa\cdot K_{ADC}\cdot K_{DAC}\cdot P_A(s)\cdot P_H(s) \quad (2)$$

the plant model in a continuous time domain, where tpa[1/rad], K_{ADC}, K_{DAC} are the scaling factor from the angle of the voice coil motor(VCM) to the relative position of the head with respect to the track on the disk, ADC gain, and DAC gain, respectively. $Z\{\cdot\}$ denotes the Z-transformation operator and $\Psi_D\{\cdot,N\}$ denotes the decimation operator by order N. Note that we used a different notation for the z-transforms, that is, "z" for the discrete time domain with a sampling time T_S and "z_2"for the discrete time domain with a sampling time $T_S/2$ to handle the effect of multi-rate notch filters. Also note that we concatenated the notch filters to the plant model instead of considering it as a part of the digital controller. This is mainly for the convenience of the analysis of the system with multi-rate notch filters.

Third, we finally verify the mathematical model by comparing it with the real measurement data. Fig.3 shows the *Bode* plot of the open-loop system using the mathematical model and the measurement data. We can see that the mathematical model is quite close to the real system.

2.3 Estimation of a Disturbance

As shown in Fig.1, the true PES y, is related to r, w, and n by the following expression.

$$y = G_{ry}r + G_{wy}w + G_{dy}d + G_{ny}n \quad (3)$$

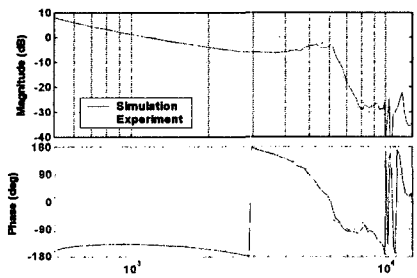

Fig. 3 Bode plot of the open-loop : xperiment(dotted) and simulation(solid)

where G_{ry}, G_{wy}, G_{dy}, and G_{ny} represent the transfer function from r to y, w to y, d to y, and n to y,respectively. Since $r = 0$ during the track following, we will disregard r from now on. In addition, the measurement noise n is assumed to be AWGN(Additive White Gaussian Noise) and is independent of r, w, and d.

After some mathematical manipulations, we can easily show that the measured PES

$$y_m(k) = y(k) + n(k) \tag{4}$$

can be expressed as follows.

$$y_m(z) = S(z)\, d^*(z), \tag{5}$$

where

$$\begin{aligned} d^*(z) &= G_P(z)w(z) + d(z) + n(z) \\ S(z) &= \frac{1}{1 + C(z)G_P(z)} \end{aligned} \tag{6}$$

are the position mode equivalent total disturbance and the sensitivity function, respectively. It is easy to show that the original system shown in Fig.1 is equivalent to the system in which d is replaced by d^* with $w=n=r=0$. We will identify d^* instead of identifying w, d, and n individually[3]. For simplicity, we continue to write d for d^* and set $w=n=r=0$ for concept development. Using (5) and (6), we can see that the position mode equivalent total disturbance d can be identified from the following equation[3].

$$d(z) = S(z)^{-1}\, y_m(z) \tag{7}$$

On the other hand, PES has two components, a repeatable run-out(RRO) y_{RRO} synchronized with the disk rotation and a non-repeatable run-out(NRRO) y_{NRRO}. That is, $y = y_{RRO} + y_{NRRO}$. In order to identify the RRO component, we first collect a PES for multiple revolutions(P) and multiple iterations(Q), and average it for each sector, that is,

$$y_{RRO}^S(k) = \frac{1}{PQ}\sum_{p=1}^{P}\sum_{q=1}^{Q} y_m^{p,q}(k), \qquad k = 1,2,\cdots,S_N \tag{8}$$

where S_N is the number of the servo sectors and $y_m^{p,q}(k)$ represents the measured PES at sector number k, p-th revolution, and q-th iteration. Note that by choosing P and Q large enough, we can filter out the effect of the measurement noise n and the NRRO since it is not repeatable. By definition, RRO is repetitive, hence we can extend the $y_{RRO}^S(k)$ to the whole period of time by repeating the sequence $y_{RRO}^S(k)$, which is defined only for a finite time. That is,

$$y_{RRO}(k) = y_{RRO}^S(\mathrm{mod}(k-1, S_N) + 1), \qquad k = 1,2,\cdots \tag{9}$$

where *mod* represents modulus operator.

By definition, y_{NRRO} is given by $y_{NRRO} = y - y_{RRO}$. On the other hand, from the relation (4), the reduction of the measured PES, y_m implies the reduction of the true PES, y since the measurement noise n is independent of the other signals. Therefore, we assume that PES means the measured PES y_m, hereafter. Similarly, we can decompose the disturbance d by a repeatable one, d_{RRO} and a non-repeatable one, d_{NRRO}. That is, from(7),

$$\begin{aligned} d_{RRO}(z) &= S(z)^{-1}\, y_{RRO}(z) \\ d_{NRRO}(z) &= S(z)^{-1}\, y_{NRRO}(z) \end{aligned} \tag{10}$$

Note that the direct inversion of the system is impossible since, in general, the $S(z)$ is not minimum phase and thus the inverse system is not realizable. To avoid this, a stable inversion technique via a projection of unstable poles to the stable ones, is sometimes used but it also has some limitations[3]. Instead, we use a frequency domain inversion and the PES is also estimated in the frequency domain. From the well-known *Parseval*'s theorem,

$$\sum_{k=0}^{N-1} |a_k|^2 = \frac{1}{N}\sum_{n=0}^{N-1} |x(n)|^2 = \sigma_x^2 \tag{11}$$

We can see that the averaged power spectral density or the absolute squared sum of the *Fourier* coefficients is equal to the average squared value of the time history[5]. Note that it is nothing but the variance if zero-mean is assumed. Thus, instead of calculating the PES level using a time history, we will evaluate the PES level in the frequency domain using the *Fourier* coefficients.

In Fig.4, the magnitude of the *Fourier* coefficients of the d, d_{RRO}, and d_{NRRO} are shown. For the estimation of

the disturbance, we have used a PES for 60 revolutions with 5 iteration using 2 HDD's with 4 heads. We have also found that the frequency spectrum is quite identical for each trial when we repeated the experiment several times. Thus, we can see that the large but finite number of samples are quite sufficient to characterize the frequency spectrum of the disturbance. This equivalence will be verified again in chapter 4[4].

2.4 Controller Design

For the track-following controller, a PID controller or state-feedback with state-observer is generally used[2],[3]. In addition, single/multi-rate notch filters, RRO compensator such Adaptive Feed-Forward Compensator(AFC), and power amplifier also affect the TMR[6]. However, a RRO compensator, notch filters, power amplifier can be designed almost independently of the main feedback controller. To design all the above controllers is beyond the scope of this paper and thus we assume that the controller is fixed. We use a state-space compensator of 5th order for the track following controller, that is,

$$C(z) = C(z, k_1, k_2, l_1, l_2, l_3) \qquad (12)$$

where k_1 and k_2 are the state feedback gains and l_1, l_2, and l_3 are the state estimator gains.

For the stability of the overall system, the stability margin such as gain margin(GM) and phase margin(PM) from the classical control theory has been widely used for the HDD servo systems[2]-[4]. In addition to that, we add a new stability concept, which is more suitable for the HDD servo system; sensitivity peak at the high frequency region(SPH) defined as

$$\mathrm{SPH}\ (G, \omega_H) \equiv \sup_{\omega > \omega_H} \left\| \frac{1}{1 + G(j\omega)} \right\| \qquad (13)$$

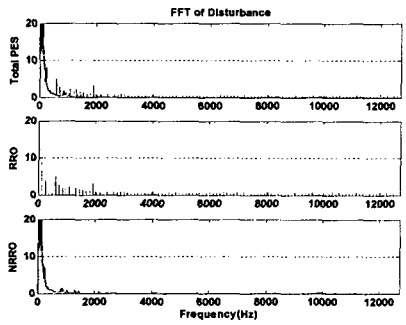

Fig. 4 Frequency spectrum of the disturbance : total(top), RRO(middle), and NRRO(bottom)

By definition, it is the peak value of the sensitivity function at the frequency above ω_H but it also represents the distance from $G(j\omega)$ to the point (-1,0), which is similar to the *vector margin*[1].

Various kinds of calibration techniques are widely used to compensate the mismatch between the desired gains and the actual ones for the rigid body motion[7]. However, no suitable method has been proposed to compensate the model mismatch for the high frequency resonance modes. See Fig.1 to see the model mismatch problem. For this reason, we consider the GM, PM, and SPH with ω_H=7kHz for the stability margin.

3. Main Result

3.1 Statement of a Problem

As is stated in chapter 1, we use a number of drives and heads to design a controller which yields the minimum PES and is robust to the variation of the plant model. For this purpose, we define a new stability concept to deal with our optimization problem with robustness.

Definition 1 (Robust Stability) :

Consider the system as in Fig.1. Let a set of plant models $\boldsymbol{P}$, a controller $C(z)$, and a stability margin $\boldsymbol{M_S}$ = $[G_M, P_M, S_{PH}]$ be given. Let $S(p,C)$ be the system in Fig.1 with the $P_H = p$ and the controller C. Then, the controller C is said to be robust M_S stable over $\boldsymbol{P}$ if for all $p \in \boldsymbol{P}$,

(i) $\mathrm{GM}(S(p,C)) \geq G_M$
(ii) $\mathrm{PM}(S(p,C)) \geq P_M$
(iii) $-\mathrm{SPH}(S(p,C)) \geq -S_{PH}$

where GM(S), PM(S), and SPH(S) represent gain margin, phase margin, and SPH of the system S.

Now, we are ready to state formally our optimization problem considered in this paper.

Problem :

Consider an HDD servo system as shown Fig.1. Let a set of plant models $\boldsymbol{P}$, a set of stability margin constraints $\boldsymbol{M_S}$, a set of bounds in controller parameters $\boldsymbol{B_G}$, and a disturbance d are given. Let $\boldsymbol{B_S}(\boldsymbol{M_S}, \boldsymbol{P}) \subset \boldsymbol{R^5}$ be the set of all $x \in \boldsymbol{R^5}$ such that $x \in \boldsymbol{B_S}(\boldsymbol{M_S}, \boldsymbol{P})$ implies $C(z,x)$ is robust M_S stable over $\boldsymbol{P}$. Then, find an $x^* = [k_1^*, k_2^*, l_1^*, l_2^*, l_3^*] \in \boldsymbol{B_G} \cap \boldsymbol{B_S}(\boldsymbol{M_S}, \boldsymbol{P}) \subset \boldsymbol{R^5}$ such that

$$F(x^*, P) \leq F(x, P) \quad \text{for } \forall x \in B_G \cap B_S(M_S, P) \subset R^5 \qquad (14)$$

where

$$F(x,P) \equiv \underset{p\in P}{\text{avg}}\left\{\sqrt{E\left[|y(\cdot,x,p)|^2\right]}\right\} \qquad (15)$$

and $y(\cdot, x, p)$ denotes the sequence of PES with the plant model $P_H(s)=p$ and the controller $C(z)=C(z, x)$.

Before closing this section, we add some comments on the formulation of our optimization problem. First, the set of plant models P is composed of the fitted mathematical models of the HDA's for a number of drives and heads to give a kind of robustness to our controller. Second, for the stability margin, we consider the worst case stability, that is, the stability margin should be satisfied for all the plant models or for all the drives and heads while the PES level is calculated in an average sense. Third, we limit the bound for the controller parameters. This is only for the efficiency of the numerical search algorithm and thus does not limit the minimum PES level. Finally, in calculating the averaged PES, we have used a frequency domain estimation using (5) and (11), i.e.

$$E\left[|y(\cdot,x,p)|^2\right]=\frac{1}{N}\sum_{k=0}^{N-1}\left|S(e^{j2\pi k/(NT_s)},x,p)\cdot d(e^{j2\pi k/(NT_s)})\right|^2 \qquad (16)$$

Similarly, y_{RRO} and y_{NRRO} can be calculated with d replaced by d_{RRO} and d_{NRRO}, respectively.

3.2 Optimization via RRNS

In this section, we propose a numerical search algorithm so-called *robust random neighborhood search*(RRNS) algorithm, which will be used to solve our optimization problem. Note the RRNS algorithm is almost free from the huge computational burden in a binary search method or a local minimum problem of the gradient search method since it searches the optimal value quite randomly and adaptively changes the search bound. The detailed algorithm is shown below.

RRNS Algorithm :

(i) Set $k=0$, $x_{OPT}=x_0$, $r=r_0>0$, and $y_{OPT}=\infty$.
(ii) Set $k=k+1$ and $x=x_{OPT}+r\cdot rand()$.
(iii) Test if $C(z,x)$ is robust M_S stable over P.
If no, increase r and go to (iv).
If yes, test if $F(x,P) < y_{OPT}$.
If no, increase r and go to (iv).
If yes, set $x_{OPT}=x$, $y_{OPT}=F(x,P)$,
decrease r, and go to (iv).
(iv) Test if $k \geq MaxIter$.
If yes, save x_{OPT} and y_{OPT} and exit.
If no, go to (ii).

Table 1 System Parameters and PES data before and after optimization

Item	Unit	Before Optimization		After Optimization	
		Simulation	Experiment	Simulation	Experiment
Total	Track[%]	3.16	3.11	2.95	2.87
RRO	Track[%]	1.93	1.93	1.84	1.72
NRRO	Track[%]	2.52	2.42	2.32	2.30
GM	dB	5.6	5.5	5.0	5.0
PM	deg	38	39	41	42
BW	kHz	1.15	1.17	1.29	1.25
SPH	dB	1.2	1.3	1.7	1.2

4. Simulation and Experimental Result

In this chapter, we demonstrate the excellent performance of the proposed design scheme through simulation and experiment. In our simulation and experimental work, we have used two HDD's which have four heads and 115,000/inch TPI. The number of servo sectors is 212 and the rotational speed is 7,200 rpm, which corresponds to the sampling rate of 25.44kHz.

During the optimization, we have used the stability margin M_S = [G_M, P_M, S_{PH}]=[5dB, 33deg, 2dB], MaxIter = 200, and r_0=0.5. In the RRNS algorithm, the *"rand"* represents a random vector whose component is a random number which is uniformly distributed over [-0.5, 0.5]. We have tried the optimization several times and obtained almost same result for every trial, which confirms the RRNS algorithm is free from the local minimum problem.

The simulation and experimental results are summarized in Table.1. The PES level is given in an averaged percent(%) track width using 1-sigma. Note that for the PES estimation, we have used an averaged power spectral density in the frequency domain for simulation results while an average of the absolute squared value of the time history is used for experimental results. Although it is not shown here, we have found that for the experimental result, the evaluation of the PES level in the frequency domain and time domain is almost identical. This demonstrates the identity in (16) holds for a sequence having long but finite interval. As shown in Table.1, the standard deviation of the total PES has reduced by 9% while all the stability margins are guaranteed. In addition, we can also see that the simulation result is quite close to the experimental one and thus it is confirmed once again that the mathematical model we have derived matches well with the real system. For better understanding of the optimized controller, the averaged spectrum of PES before and after

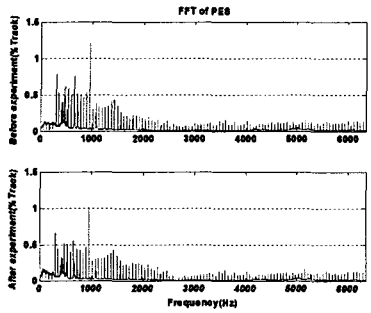

Fig. 5 Averaged frequency spectrum of the PES before(top) and after(bottom) optimization

optimization is shown in Fig.5. As shown in the figure, the PES spectrum is reduced especially in the low frequency region that is mainly due to the increase of the bandwidth. However, we can also see that the degradation of the stability margin is almost negligible. We can obtain a similar result even if we use all the same bandwidth for the nominal gain although the reduction ratio might be a little decreased. Detailed result is omitted here because of the limited space.

5. Conclusion

In this paper, we have described a new design procedure which is systematic as well as more accurate than the current design practice. In addition, we optimized the controller parameters via RRNS optimization process which yields a minimum PES level while the stability with respect to the variation of the plant model is guaranteed. We have also demonstrated that the mathematical model derived is quite close to the real system, which implies that the design and verification can be done via simulation instead of experiment. Hence the development time will be reduced and the design cost will also be significantly saved.

References

[1] G. F. Franklin, J. D. Powell, and A. Emami-Naeini, 1991, Feedback Control of Dynamic Systems, 2nd Edition, Addison-Wesley

[2] G. F. Franklin, J. D. Powell, and M. L. Workman,1990, Digital Control of Dynamic Systems, 2nd Edition, Menlo Park : Addison-Wesley

[3] H. S. Lee., October 2001, "Controller Optimization for Minimum Position Error Signals of Hard Disk Drives," IEEE Transactions on Industrial electronics, Vol.48, No. 5, pp.945-950

[4] Y. H. Kim, D. H. Oh, and H. S. Lee., February 2005, "PES Reduction in Magnetic Disk Drives via a Low-TMR HGA and Servo Loop Shaping," IEEE Transactions on Magnetics, Vol.41, No.2, pp.779-783

[5] R. E. Crochiere and L. R. Rabiner,1983, Multirate Digital Signal Processing, Englewood Cliffs, NJ : Prentice-Hall

[6] A. H. Sacks, M. Bodson, and W. Messner, March 1995, "Advanced Methods for Repeatable Runout Compensation," IEEE Transactions on Magnetics, Vol. 31, No.2

[7] C. I. Kang, "Method of estimating gain of servo control system", U.S. Patent. No. US5969494.